4.1. Introduction

In the past few decades, the science and technology of nanomaterial have been speedily advancing. The development of various synthesis methods has presented many challenges regarding the control of size and shape of nanoscale materials by changing the synthesis procedures. The composite materials exhibiting a high dielectric constant are either perovskite-based ferroelectric ceramics such as undoped or doped $BaTiO_3$ or the relaxor ferroelectrics including $Pb(Mg_{1/3}Nb_{2/3})O_3$[PMN], $Pb(Zn_{1/3}Nb_{2/3})O_3$[PZN] and $Pb_{1-x}La_x(Zr_{1-y}Ti_y)O_3$ [PLZT] [Patrinoiu *et al*. (2012), Jie *et al*. (2004), Zhang *et al*. (2011), Yang *et al*. (2014)]. Dielectric and ferroelectric ceramic materials have potential interest as a field of solid-state electronics. The major applications for dielectric ceramic are as electrical insulation in electronic circuits and as capacitive elements. Electric power storage plays a critical role in mobile electronic devices, stationary power systems, hybrid electric vehicles, pulse power applications, etc. [Nalwa (1999), Osaka & Datta *et al*. (2001)]. Moreover, no relation to the dielectric properties of the material has been established. More work on the topic is needed, since the understanding of this anomaly may offer an alternative and powerful way of controlling the nanostructure and modifying the dielectric response of $BaTiO_3$ based materials just by modification the sintering temperature. $BaTiO_3$ (BTO) Ceramics have a prominent interest in a broad range of applications in microelectronics, namely, in tunable microwave devices due to the high dielectric constant $\varepsilon' > 1000$ due to its ferroelectric nature [Barber *et al*. (2009)]. The addition of lead titanate in small percentages appears to render the remanent polarization of $BaTiO_3$ permanent [Marks & Monson *et al*. (1955)]. On the other hand, the complex perovskite $CaCu_3Ti_4O_{12}$ (CCTO) has a giant dielectric constant ($\varepsilon' \sim 10^4$) at room temperature, which is independent of temperature (100–600 K) and frequency below 10^6 Hz [Subramanian *et al*. (2000), Ramirez *et al*. (2000)]. The high dielectric constant has

been attributed to inter-barrier layer capacitance (IBLC) formation at grain boundaries. [Lunkenheimer *et al*. (2002), Lunkenheimer *et al*. (2004) Liu *et al*. (2004), Sinclair *et al*. (2002)]. In CCTO, dielectric constant and dielectric loss increase proportionally, indicating that the process of energy storage is related to the conduction mechanisms. Due to the novel composite performance, such as the coexistence of ferroelectric and ferromagnetic properties and the improvement of magneto-electric (ME) coupling effect, the research on multi-ferroic ME composite materials has become an attractive hot topic in recent years [Ryu *et al*. (2002), Zheng *et al*. (2004)]. Therefore, the challenge is to create a material with high energy storage without a considerable increase in dielectric loss, to enhance dielectric permittivity and dielectric field strength. The development of the various synthesis of nano-scale material has presented many challenges regarding the control of size and shape by varying the synthesis procedures [Jie *et al*. (2004), Zhang *et al*. (2011), Patrinoiu *et al*. (2012)].

In the present work, we are reporting a systematic study of $0.9CaCu_3Ti_4O_{12}$ – $0.1BaTiO_3$ (CC-BT) nanocomposite has been synthesized using the modified solid state route. The above composite has been successfully prepared by a very simple and modified solid state route without using very expensive oxynitrate, alkoxide or titanium chloride. We investigated the characteristics of CC-BT nanocomposite. The resulting composite was characterized by XRD, SEM, TEM and their dielectric properties were also reported.

4.2. Experimental

4.2.1. Synthesis

The composite ceramic of $0.9CaCu_3Ti_4O_{12}$–$0.1BaTiO_3$ (CC-BT) was synthesized by solid-state method via three steps. Firstly $CaCu_3Ti_4O_{12}$ (CCTO) was synthesized by

semi wet route using analytical grade $Ca(NO_3)_2.4H_2O$ (99.5% Merck, India), $Cu(NO_3)_2.3H_2O$ (99.8% Merck, India), Solid TiO_2 (99.5% Merck, India), as the starting materials. In this route, their stoichiometric amounts were mixed in a beaker along with solid TiO_2. Secondly, $BaTiO_3$ (BTO) was also prepared by a semi-wet process using $Ba(NO_3)_2.TiO_2$ (99.7% Merck, India), and citric acid (99.5% Merck, India) as the starting materials. In this route, their stoichiometric amounts were mixed in a beaker along with solid TiO_2, and then citric acid (equivalent to metal ions) was added to the solution. The consequential solution was heated on a hot plate magnetic stirrer at 70-80 $^{\circ}$C to evaporate the water and allow self-ignition. The ignition process was carried out in the air, which exhausted a lot of gasses and created a fluffy mass of CCTO and BTO ceramic powder in two separate beakers. In this process, the mixing of a solution of a metal precursor and an organic polyfunctional acid having, at least, one hydroxyl group and one carboxylic acid group such as citric, glycine, tartaric or glycerol. Citric acid as a complexion agent can form a complex and provide the fuel for the ignition step. The dried powder of CCTO and BTO were calcined in air at 800 $^{\circ}$C for 8 h in an electrical furnace. Thirdly, the amount of the prepared powders of CCTO and BTO by a semi-wet route was mixed. In this process, we used calcined powder of CCTO and BTO as raw materials to synthesize the CC-BT composite ceramic to develop the new modified solid state route to get a nanometer range powder. The mixed CC-BT nanocomposite ceramic powder was mixed with 2 % polyvinyl alcohol (PVA) as a binder and pressed into a cylindrical pellet (10 mm × 1 mm) using a hydraulic press (4-5 tons). The PVA binder was burnt out at 500 °C for 2 h. Finally, the CC-BT nanocomposite pellets were sintered at 950 °C for 12 h.

4.2.2. Characterization

The crystalline phase of CC-BT nanocomposite sintered sample was identified by using the X-ray diffraction analysis (Rigaku, miniflex-600, Japan) employing Cu-kα radiation. The microstructures of the fractured surface of sintered ceramic were observed using a scanning electron microscope (SEM, ZEISS, model EVO18, Germany) and the particle size was evaluated using a high-resolution transmission electron microscope (TEM, Tecnai G^2 20 TWIN). The specimen for TEM analysis was prepared by dispersing the sintered CC-BT powder in acetone by ultra-sonication. The obtained suspensions were deposited on the carbon-coated copper grids. The surface morphology was analyzed by atomic force microscopy [AFM Nano Drive Dimension Edge 8.06, and Bruker]. The sample was prepared by dispersing the sintered CC-BT nanocomposite powders in acetone by ultra-sonication, and this type of suspension was deposited on the glass slides. Dielectric and electric measurements were made using a pellet which both surfaces were polished and coated with silver paint which was then dried at 200 °C for 25 minutes and cooled naturally to room temperature. The dielectric and electrical data of the CC-BT ceramic was collected using an LCR meter (PSM 1735, NumetriQ 4^{th} Ltd, and U.K) over a frequency range of 10^2–10^6 Hz and in the temperature range of 300–500 K.

4.3. Results and Discussion

4.3.1. X-ray diffraction studies

Figure 4.1 shows the X-ray diffraction patterns of CC-BT powder sintered at 950 °C for 12 h. XRD data were indexed on the basis of a cubic unit cell similar to CCTO ceramic (JCPDS card no. 75-2188) with minor phases of BTO. XRD of CC-BT patterns shows the presence of split peaks for the reflections at 440, 422 and 400 due to the presence of Cu-Ka_2 along with Cu-Ka_1 in the X-ray radiations used for the diffraction

[Culity & Stock *et al*. (2001)]. The Crystallite size (D) of the nanocomposite ceramic is also determined with the help of XRD data using line broadening method. The value of crystallite size is given by the Cauchy component of the Voigt function in the single-line analysis process. The crystallite size of the ceramic was estimated using the equaction 2.2. The average crystallite size derived from the XRD data was 34 ± 4 nm for the CC-BT composite ceramic sintered for 12 h.

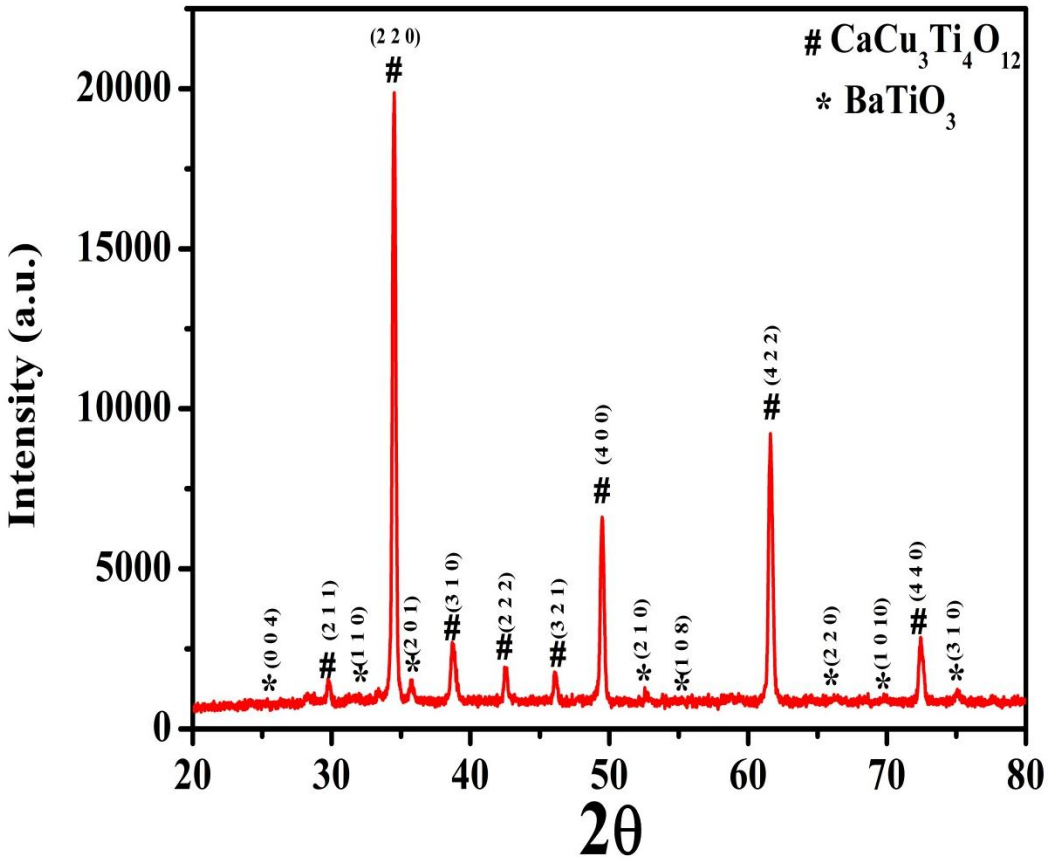

Figure 4.1 X-ray powder diffraction pattern of a CC-BT nanocomposite sintered at 950 °C for 12 h.

4.3.2. Microstructural studies

Figure 4.2(a) shows the bright field TEM image of the CC-BT ceramic sintered at 950 °C for 12 h. The particle sizes of the CC-BT ceramic was 40 ± 5 nm which is shown that the ceramic powder was found to be nanocrystalline in nature. The particle sizes observed by TEM is good agreement with XRD data. Figure 4.2(b) shows the selected area electron diffraction patterns (SAED) of the CC-BT ceramic which confirmed the polycrystalline nature of the material. The SAED pattern consists of concentric rings. The additional spots observed in the patterns were from the CCTO along with the BTO grains because of their orientation in a different direction. The indexed electron diffraction patterns also supported the cubic structure.

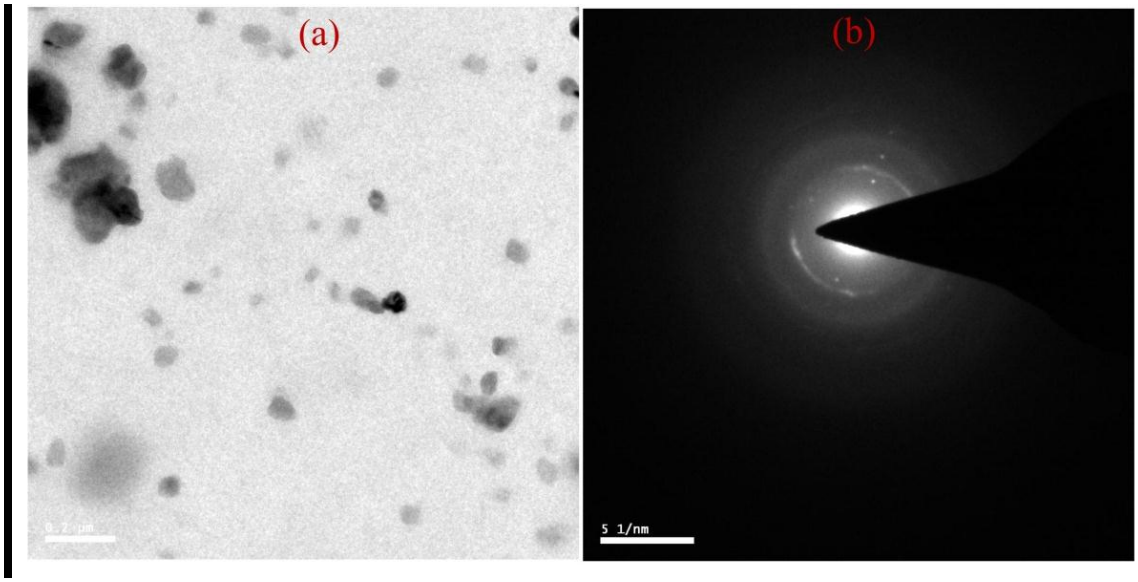

Figure 4.2. (**a)** Bright field TEM images, (**b)** SEAD pattern of a CC-BT nanocomposite sintered at 950 °C for 12 h.

Figure 4.3 shows microstructure of the fractured surface of the CC-BT nanocomposite ceramic sintered at 950 °C for 12 h. Grains having a size in the range of 1.0 – 2.0 μm are observed and indicate the presence of the bimodal distribution of grains. The junctions of grains by fracture surface can be noted, and Pure CCTO also exhibits a transgranular fracture [Rai *et al***.** (2009)]. Barium titanate undergoes phase transformation during the sintering treatment, which leads to abnormal grain growth [Kim *et al***.** (1999), Huang & Chen *et al***.** (2002)]. The AFM images of CC-BT composite ceramic sintered at 950 °C for 12 h was recorded.

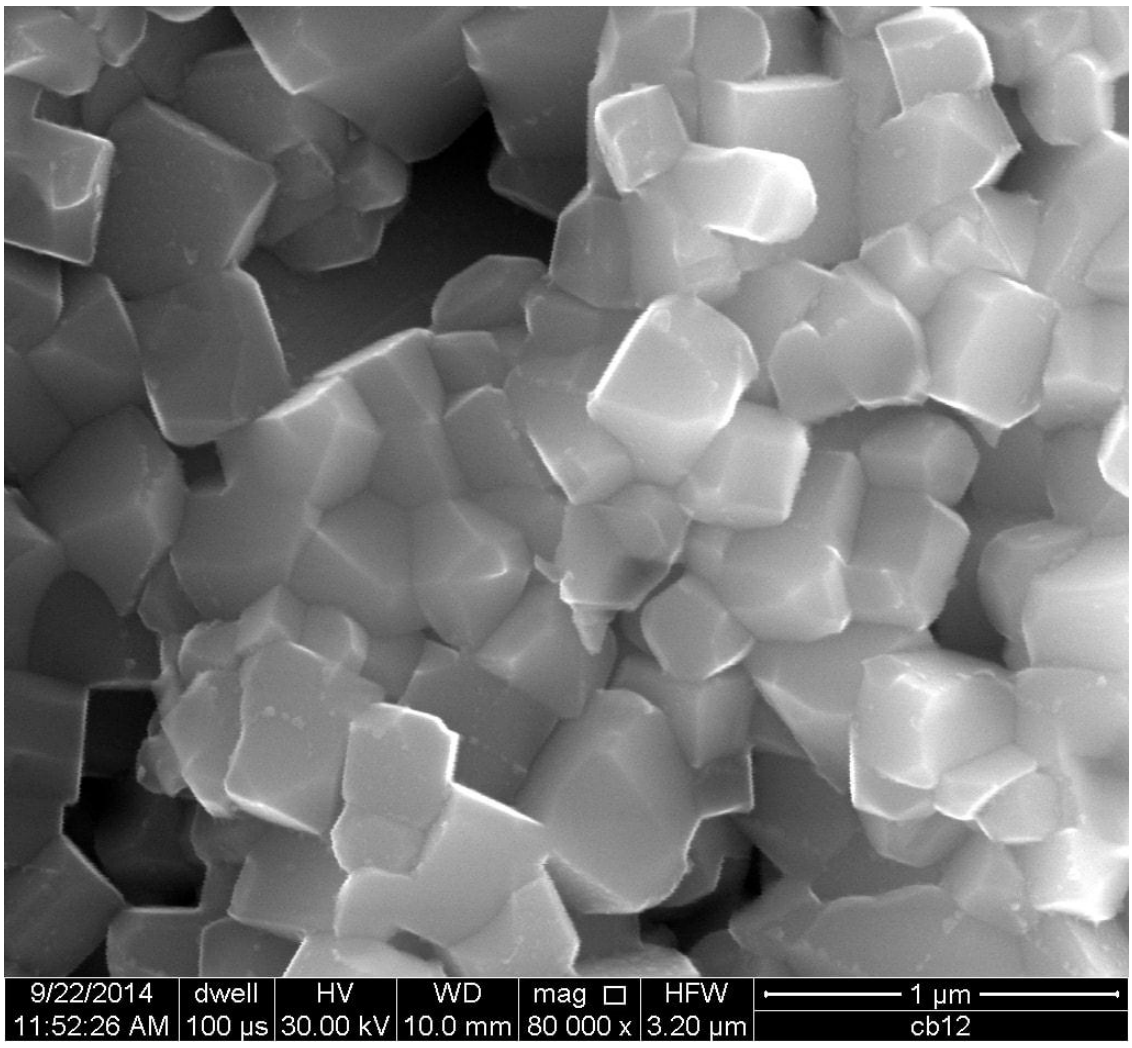

Figure 4.3. SEM image of a CC-BT nanocomposite sintered at 950 °C for 12 h.

Figure 4.4 (a) and (b) shows 2 D and 3 D images of the surface of CC-BT ceramic. The surface roughness (Rq) is calculated using following formula

$$Rq = \sqrt{\left(\sum \frac{(Zi-Zave)^2}{N}\right)} \qquad (4.2)$$

Where Rq is the surface roughness, Z_{ave} is the average of the Z values within the particular field, Z_i is the height value at that point, and N is the number of points within the given area. The Roughness R_{max}, average roughness, and root mean square (Rq) data were obtained as 2.3 um, 1.41 nm and 2.24 nm respectively on scanned area 775 nm × 775 nm. Figure 4.4 (d) showed the histogram of CC-BT and estimated the average grain size was found to be 1.0 – 2.0 μm. It supported to the size of SEM fracture surface.

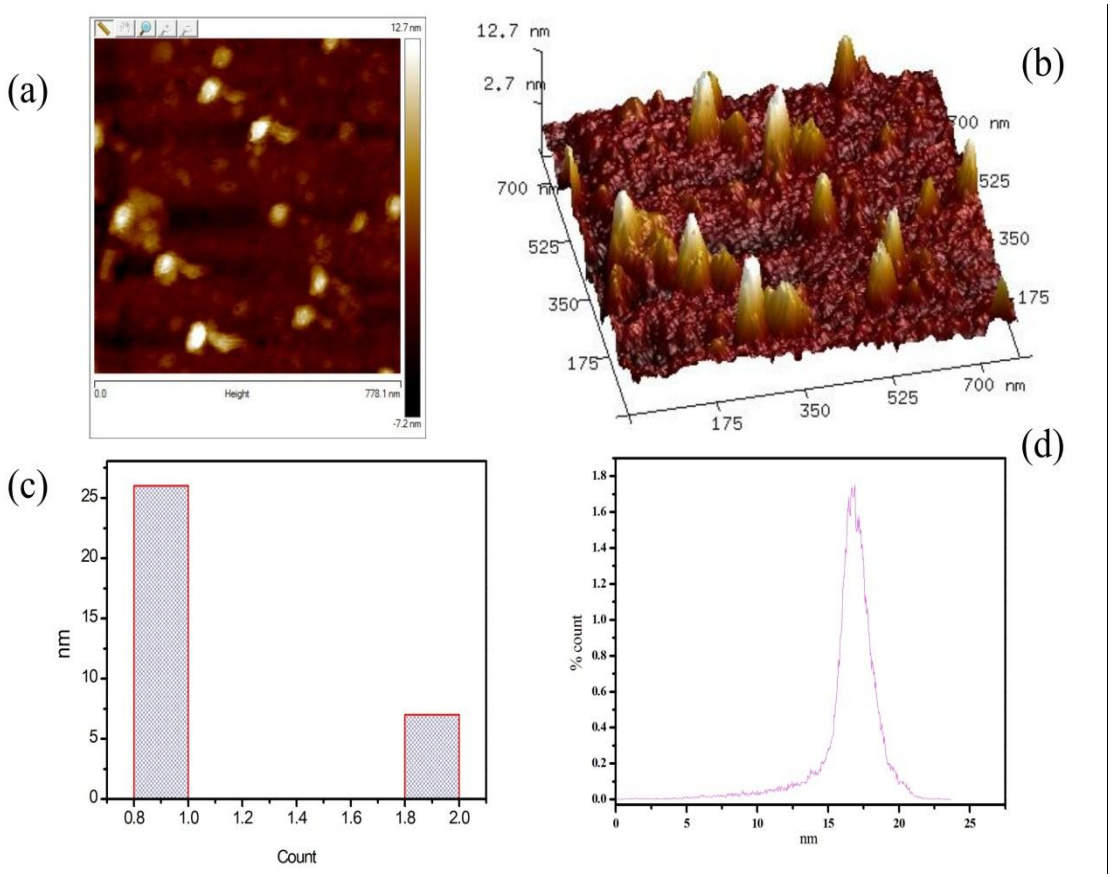

Figure 4.4. AFM images of CC-BT nanocomposite sintered at 950 °C for 12 h (**a)** 2 dimensional (**b)** 3D Structure (**c)** bar diagram of particles size and (**d)** depth histogram.

4.3.3. Dielectric Studies

Variation of dielectric constant (ε′), and dielectric loss (tan δ) with the temperature at 100 Hz, 1 kHz, 10 kHz and 100 kHz for CC-BT nanocomposite ceramic sintered at 950 °C is shown in Figure 4.5.

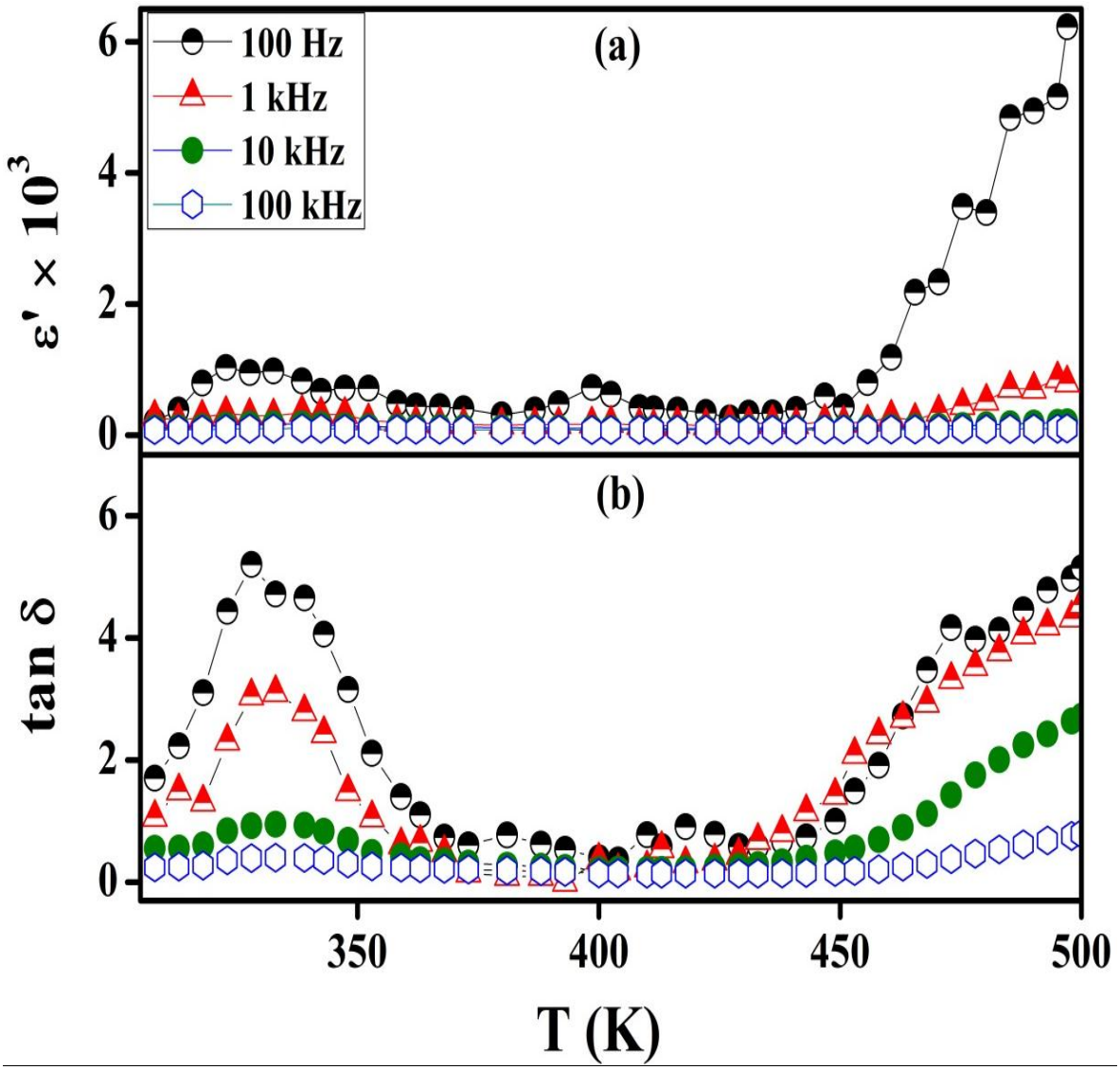

Figure 4.5. (**a)** Variation of the dielectric constant (ε′), (**b)** dielectric loss (tan δ) with temperature for the CC-BT nanocomposite at a few selected frequencies**.**

It is noted from Figure 4.5(a) that the dielectric constant of CC-BT ceramic is around 1034 at room temperature and it is almost temperature independent from 300 K to 500 K. At lower frequency (100 Hz), the dielectric constant of CC-BT composite ceramic increases rapidly up to 500 K and shows an extensive anomaly around ~ 453 K where dielectric constant increases sharply. This anomaly has been observed as a ferroelectric relaxor behavior associated with the slowing down of a dipolar phenomenon within the polar composite ceramic [Ke *et al***.** (2006), Samara *et al***.** (2003)]. From Figure 4.5(b) shows that the dielectric loss (tan δ) of CC-BT is temperature independent up to 368 K and then it increases rapidly. The constant value of the dielectric loss is found to be 0.19 at 1 kHz and 404 K. A diffuse phase transition found in the composite in the temperature range (300-375 K) which characterized a ferroelectric relaxor, and strong relaxation dispersion in loss tangent (tan δ) indicate thermally activated relaxation.

Figure 4.6(a) shows the variation of dielectric constant (ε′) as a function of frequency for the ceramic CC-BT at few selected temperatures. The Dielectric constant for CC-BT decrease rapidly below 10 kHz and then remains nearly constant between 10 kHz to 5 MHz. The value of the dielectric constant is found to be ~ 3689 at 100 Hz and 210 °C. The increase in dielectric constant (ε′) with decreasing frequency can be attributed to the contribution of charge accumulation at the interface [Abadei *et al***.** (2002)].

Figure 4.6(b) shows the plots of dielectric loss (tan δ) vs. frequency at few selected temperatures for CC-BT sintered at 950 °C for 12 h. It is observed from the figure that dielectric loss (tan δ) is frequency dependent from room temperature to 500 K. Relaxation peaks are observed which shift to higher frequency region with increasing temperature. This indicates the existence of Debye-like dielectric relaxation. It arises from the dipolar

relaxations between semiconducting CC-BT grains which are separated by insulating grain boundaries [Himanshu *et al***.** (2010)].

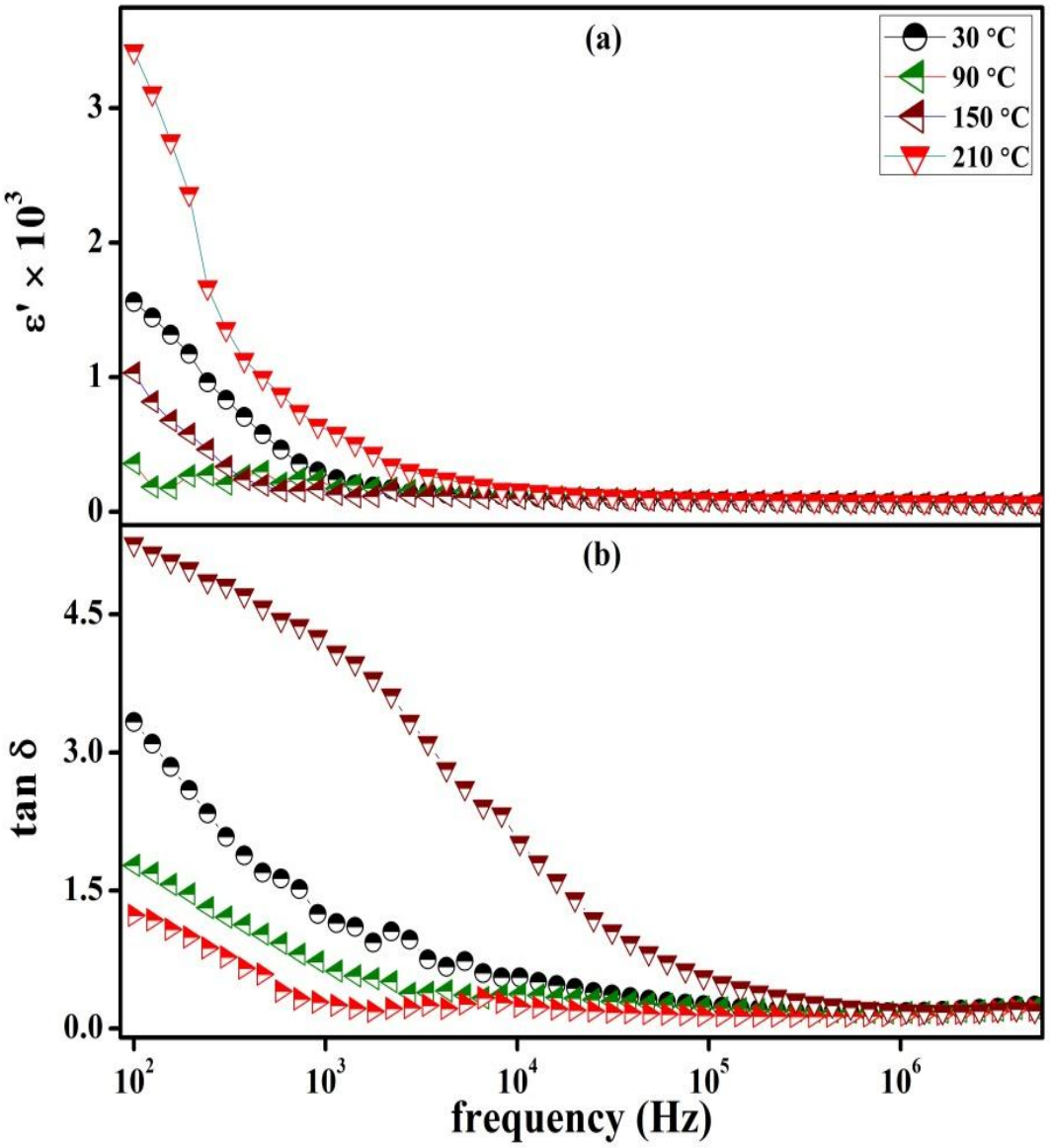

Figure 4.6. (a) Variation of dielectric constant (ε′), (**b)** dielectric loss (tan δ) with frequency for the CC-BT nanocomposite at a few selected temperatures.

4.3.4. Impedance studies

Figure 4.7 shows the variation of the real part of impedance (Z′) as a function of frequency at selected temperatures (30, 90, 150 and 210 °C). As shown, the values of Z′′ decrease with increasing temperature in the low-frequency region, and after that, they appear to be merged in the high-frequency region around 10^4 Hz follows a plateau-like behavior. At high-frequency region, the value of Z′ at each temperature coincides with each other, which is due to the possible release of space charges polarization [Kumar *et al.* (2006)]. At all temperatures, the value of Z′ decreases with increasing frequency, indicating the possibility of an increase in the AC conductivity.

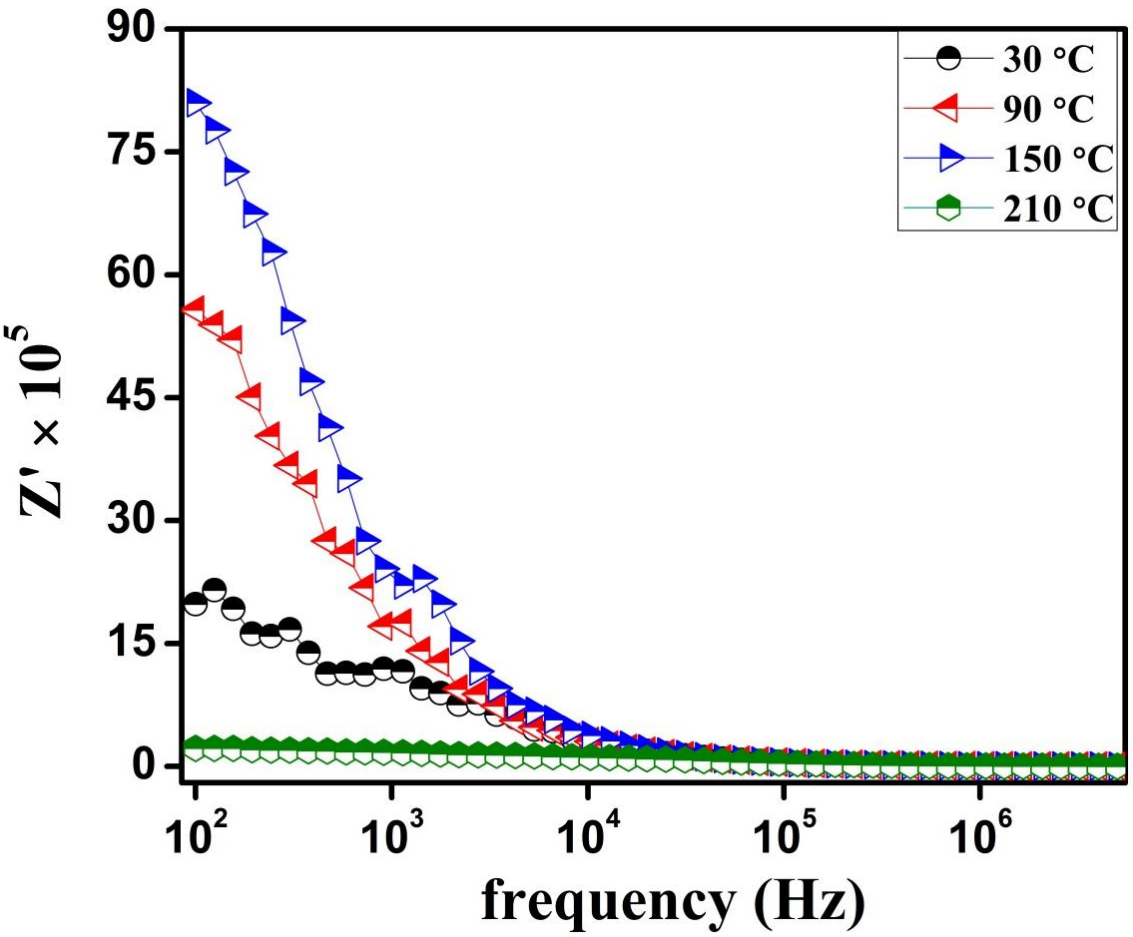

Figure 4.7. Impedance plane plots Z′ vs. frequency at a few selected temperatures of a CC-BT nanocomposite sintered at 950 °C for 12 h.

Figure 4.8 shows the presence of a semi-circular arc with different intercepts due to the grain and grain boundaries. It is shown that the resistance of the CC-BT nanocomposite decreased with Increasing temperature. The composite ceramic impedance plot depending on the relative values of relaxation time $\omega_m\tau_m = 1$, which give three semi-circular arcs [Rawat *et al*. (2012)]. Impedance spectroscopy separates the contributions of the grains and grain boundaries, and electrode specimen interface observed RC elements of the composite ceramic, respectfully [Hodge *et al*. (1976)]. The arc at the high-frequency end refers to the grain resistance, and the intermediate arc corresponds to resistance by the grain boundaries.

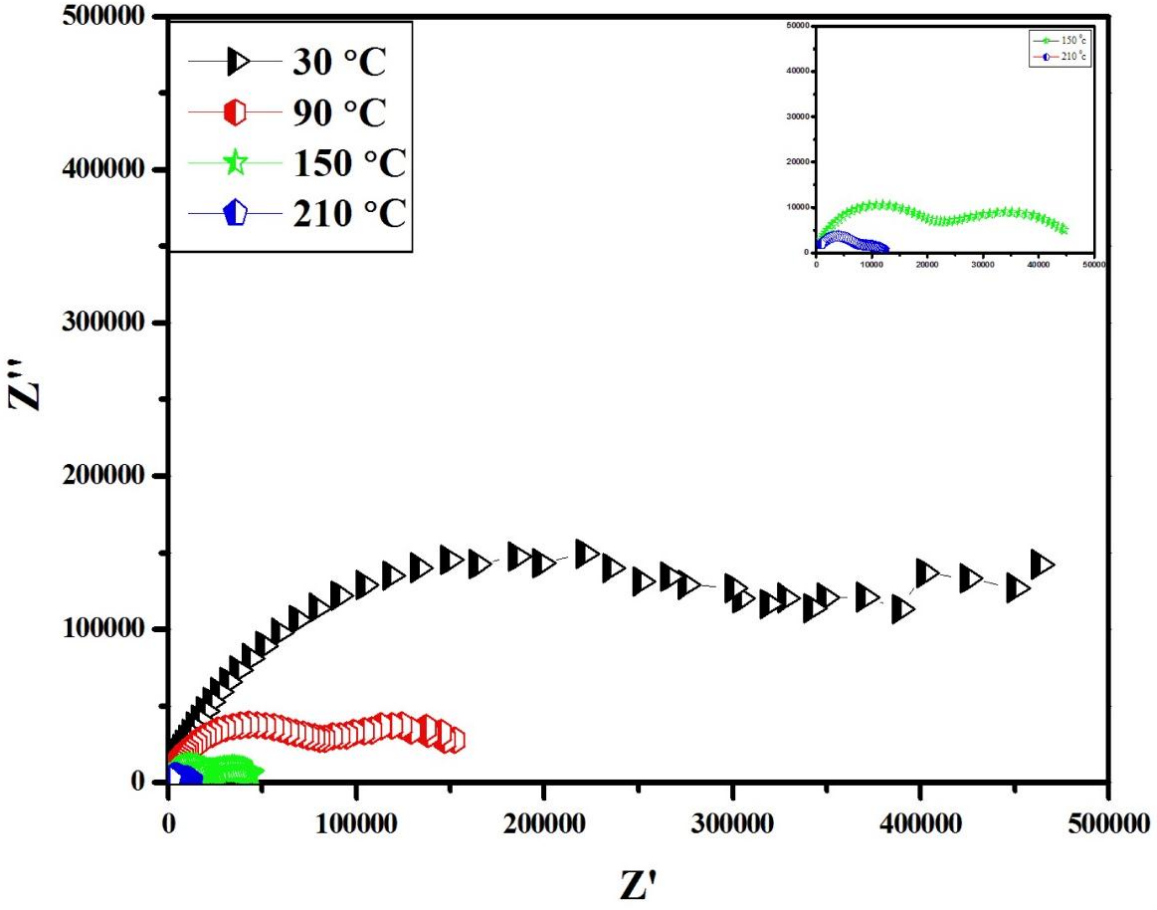

Figure 4.8. Impedance plane plots (Z′ vs. Z″) at a few selected temperatures of a CC-BT nanocomposite sintered at 950 °C for 12 h.

The of grains and grainboundaries were calculated from the Fig. 4.8. The registance of the grains was found to be 1314, 1172, 1050 and 970 Ohm at 30, 90, 150 and 210 °C respectively. The grainboundaries resistance was found found to be 6.87×10^6, 5.69×10^6, 2.34×10^6 and 1.79×10^6 Ohm at 30, 90, 150 and 210 °C respectively.

4.4. Conclusion

The modified solid state route has successfully synthesized $0.9CaCu_3Ti_4O_{12}$ – $0.1BaTiO_3$ (CC-BT) with a particle size of 40 ± 5 nm. X-Ray diffraction data confirm the presence of CCTO and BTO nanocrystalline phases co-existed in the nanocomposite. SEM and AFM studies suggest that grain boundary effects are responsible for enhanced dielectric permittivity. The CC-BT composite shows temperature-independent dielectric performance at higher frequencies region. Impedance studies confirmed that CC-BT composite is electrically heterogeneous with semiconducting grains and insulating grain boundaries. The results support IBLC mechanism which is responsible for the high dielectric constant in the CC-BT composite.